Accepted Manuscript

Title: Substrate specificity of the *Chamaerops excelsa* palm tree peroxidase. A steady-state kinetic study

Authors: Nazaret Hidalgo Cuadrado, Juan B. Arellano, Juan J. Calvete, Libia Sanz, Galina G. Zhadan, Igor Polikarpov, Sergey Bursakov, Manuel G. Roig, Valery L. Shnyrov

PII: S1381-1177(11)00245-1
DOI: doi:10.1016/j.molcatb.2011.09.005
Reference: MOLCAB 2334

To appear in: *Journal of Molecular Catalysis B: Enzymatic*

Received date: 19-3-2011
Revised date: 2-9-2011
Accepted date: 6-9-2011

Please cite this article as: N.H. Cuadrado, J.B. Arellano, J.J. Calvete, L. Sanz, G.G. Zhadan, I. Polikarpov, S. Bursakov, M.G. Roig, V.L. Shnyrov, Substrate specificity of the *Chamaerops excelsa* palm tree peroxidase. A steady-state kinetic study, *Journal of Molecular Catalysis B: Enzymatic* (2010), doi:10.1016/j.molcatb.2011.09.005

*Graphical Abstract

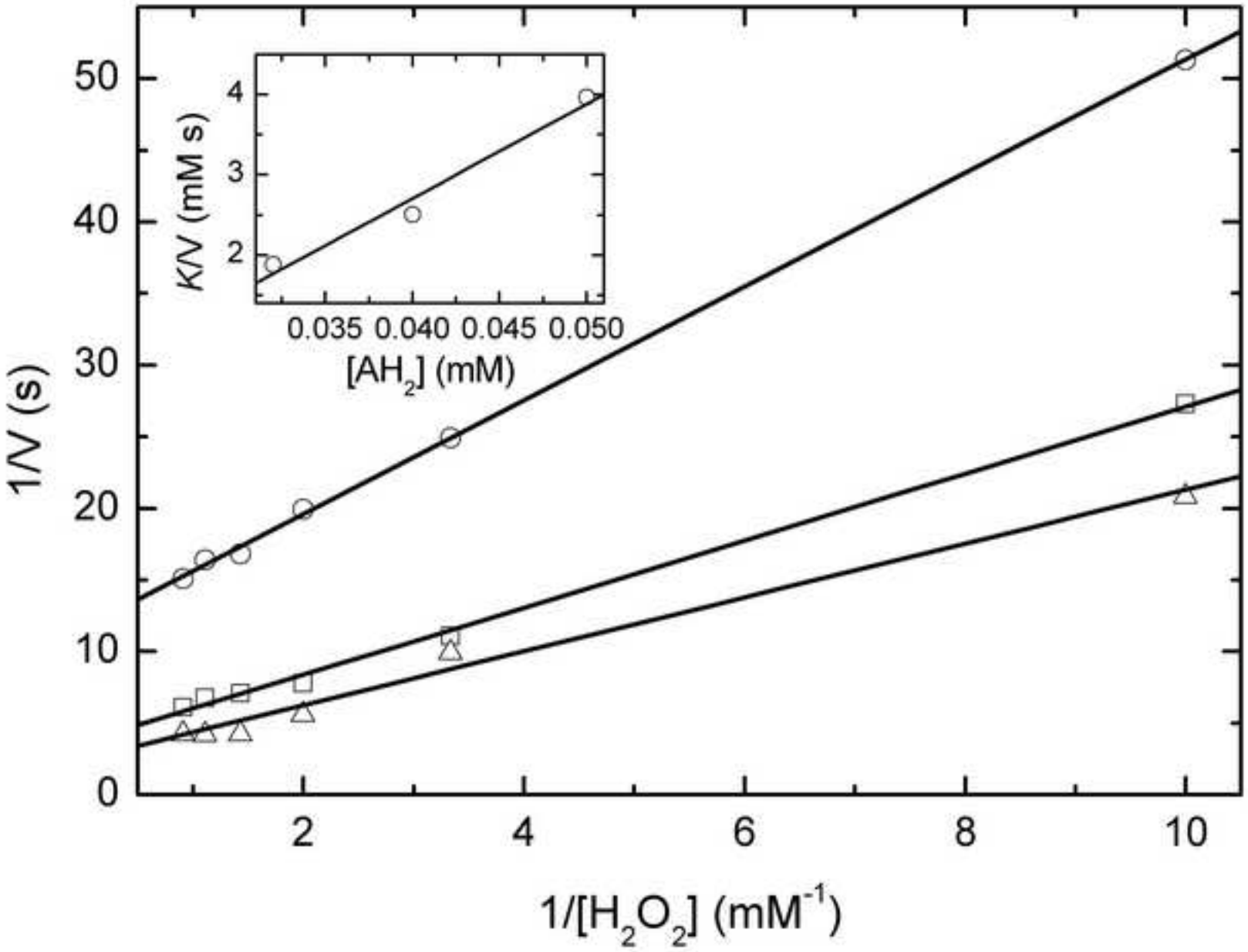

Novel Class III peroxidase biocatalyst from *Chamaerops excelsa* palm tree.

The steady state kinetic mechanism of the H_2O_2-supported oxidation of different organic substrates by this peroxidase (CEP) has been proposed.

An analysis of the initial rates *versus* H_2O_2 and reducing substrate concentrations is consistent with a substrate-inhibited Bi-Bi Ping-Pong reaction mechanism.

The corresponding kinetic parameters $K_m^{H_2O_2}$, $K_m^{AH_2}$, k_{cat}, $K_{SI}^{H_2O_2}$, $K_{SI}^{AH_2}$ and the microscopic rate constants k_1 and k_3 of the shared three-step catalytic cycle of peroxidases have been determined.

Substrate specificity of the *Chamaerops excelsa* palm tree peroxidase. A steady-state kinetic study

Nazaret Hidalgo Cuadrado[a], Juan B. Arellano[b], Juan J. Calvete[c], Libia Sanz[c], Galina G. Zhadan[d], Igor Polikarpov[e], Sergey Bursakov[f], Manuel G. Roig[a,*], Valery L. Shnyrov[d,*]

[a] *Departamento de Química Física, Facultad de Química, Universidad de Salamanca, Salamanca, Spain*

[b] *Instituto de Recursos Naturales y Agrobiologia (IRNASA-CSIC), Salamanca, Spain*

[c] *Instituto de Biomedicina de Valencia (CSIC), Valencia*

[d] *Departamento de Bioquímica y Biología Molecular, Facultad de Biología, Universidad de Salamanca, 37007 Salamanca, Spain*

[e] *Grupo de Biotecnologia Molecular, Instituto de Fisica de Sao Carlos/IFSC, Universidade de Sao Paulo/USP, Sao Carlos, Brasil*

[f] *Departamento de Protección Ambiental, Estación Experimental del Zaidin (EEZ-CSIC), Granada, Spain*

*Corresponding authors. Tel.: +34 923294487; fax: +34 923294579.

E-mail addresses: mgr@usal.es, shnyrov@usal.es

Abstract

The steady state kinetic mechanism of the H_2O_2-supported oxidation of different organic substrates by peroxidase from leaves of *Chamaerops excelsa* palm trees (CEP) has been investigated. An analysis of the initial rates *vs.* H_2O_2 and reducing substrate concentrations is consistent with a substrate-inhibited Bi-Bi Ping-Pong reaction mechanism. The phenomenological approach expresses the peroxidase Ping-Pong mechanism in the form of the Michaelis-Menten equation and leads to an interpretation of the effects in terms of the kinetic parameters $K_m^{H_2O_2}$, $K_m^{AH_2}$, k_{cat}, $K_{SI}^{H_2O_2}$, $K_{SI}^{AH_2}$ and of the microscopic rate constants k_1 and k_3 of the shared three-step catalytic cycle of peroxidases.

Keywords: *Chamaerops excelsa*; Peroxidase; Reaction Mechanism; Steady-State Kinetics; Substrate Specificity; Inhibition.

1. Introduction

Peroxidases (EC 1.11.1.7; donor: hydrogen peroxide oxidoreductase) are enzymes that are widely distributed in the living world ant that are involved in many physiological processes. The oxidation of many biological substances in body fluids produces a certain amount of hydrogen peroxide. In this sense, although the function of peroxidases is often seen primarily in terms of causing the conversion of toxic H_2O_2 to H_2O, this should not be allowed to obscure their wider participation in other reaction, such as cell wall formation, lignification, the protection of tissues from pathogenic microorganisms, suberization, auxin catabolism, defense, stress, etc [1].

In addition to their biological functions, peroxidases are important from the point of view of many biotechnological applications. This group of enzymes, in particular those from plants, enjoys widespread use as catalysts for phenolic resin synthesis [2,3] as indicators for food processing and diagnostic reagents [4,5], and as additives in bioremediation [6,7]. Under specific conditions, the radicals formed can break bonds in polymeric materials, resulting in their destruction [8].

Peroxidases reduce hydrogen peroxide and oxidize a broad number of compounds including phenols, aromatic amines, thiosanisoles, halide and thyocianate ions, fatty acids. Selectivity towards reducing substrates depends on the type of peroxidase [9]. It is quite difficult to determine which substrates are physiologically relevant for plant peroxidases owing to their ability to oxidize a broad variety of organic an inorganic substrates [8].

Peroxidases have been identified throughout the plant kingdom but that from horseradish root (HRP), and in particular the slightly basic C isoenzyme (HRPC), has been the one most thoroughly investigated. Despite this, in recent years more data have become available regarding peroxidases from other plants, such as peanut [10], barley [11], tea [12], *Arabidopsis thaliana* [13], and palm trees [14-18].

The shared three-step catalytic cycle of peroxidases, involving different intermediate enzyme forms, is known as Poulos-Kraut mechanism [19,20]. Catalysis is initiated by the binding of H_2O_2 to the high-spin ferric haem iron of resting peroxidase, followed by the heterolytic cleavage of the peroxide oxygen-oxygen bond under the influence of highly conserved histidine and arginine residues in the active site [21]. The haem undergoes a two-electron oxidation to form an intermediate (compound I) containing an oxyferryl species (Fe(IV)=O) and a porphyrin π–cation radical. A water molecule is generated as the co-product of the reaction. Completion of the catalytic cycle most often consists of two successive single-electron transfers from separate reducing substrate molecules to the enzyme. The first reduction, of the porphyrin π–cation radical in compound I, yields a second enzyme intermediate, compound II, which retains the iron in the oxyferryl state [22]. Reduction of compound II, to recover the ferric enzyme, is often rate-limiting under steady-state conditions. Extremely reactive free radicals released from the catalytic cycle quite often condense spontaneously, giving rise to polymers.

The peroxidase cycle is generally considered irreversible. However, there is no doubt that adsorption complexes between the enzyme and its substrates exist physically [23]. The microscopic constants governing the equilibrium between aromatic compounds and peroxidase have been estimated. Even though the presence of the co-substrates (donor or H_2O_2) in the enzyme modulates affinity for the other, the mechanism may proceed via random binding. This

finding, together with retain special kinetic features [24], supports the notion that there is no need for the peroxide to bind to the enzyme prior to donor adsorption.

In this work, the kinetic mechanism of the H_2O_2-supported oxidation of different organic substrates by means of a novel plant peroxidase from *Chamaerops excelsa* palm tree (CEP) has been investigated.

Among the broad variety of organic and inorganic substrates of peroxidases, here four organic substrates were studied: the chromogenic substrates guaiacol (2-metoxiphenol) and ABTS, often used as reference substrates, and o-dianisidine and o-phenylendiamine, the latter three suitable for use in ELISA procedures that employ peroxidase conjugates [25-28].

Since these oxidation reactions exhibit Michaelis-Menten saturation kinetics with respect to both substrates, the system was amenable to steady state kinetic experiments, which were used to deduce the kinetic mechanism of the reaction following the methodologies established for two-substrate enzyme systems [29]. The results of the initial rate and inhibition studies carried out here indicate that the H_2O_2-supported oxidation of different organic substrates catalyzed by this peroxidase proceeds via a Ping-Pong mechanism mediated by the oxidized enzyme intermediate compounds I and II.

2. Experimental

2.1. Materials

Analytical or extra-pure grade polyethyleneglycol (PEG), guaiacol (2-methoxyphenol), ammonium sulfate, sodium phosphate and Tris-HCl were purchased from Sigma Chemical Co. (St. Louis MO, USA) and were used without further purification. H_2O_2 was from Merck (Darmstadt, Germany). Superdex-200 columns and Phenyl-Sepharose CL-4B columns were from GE Helthcare Bio-Sciences AB (Uppsala, Sweden). TSK-Gel DEAE-5PW was purchased

from Tosoh Co. (Tokyo, Japan). Cellulose membrane tubing for dialysis (avg. flat width 3.0 in) was purchased from Sigma Chemical Co.; slide A-lyzer dialysis cassettes (extra-strength, 3-12 mL capacity, 10.000 MWCO) were form Pierce Biotechnology, Inc. (Rockford, IL, USA) and filter devices (Amicon Ultra Cellulose 10.000 MWCO, 15 mL capacity) were from Millipore Corp. (Billerica, MA, USA). All other reagents were of the highest purity available. The water used for preparing the solutions was double-distilled and then subject to a de-ionisation process.

2.2. Enzyme purification

CEP was purified from palm tree *Chamaerops excelsa* as described [15,17] but with essential modifications. Leaves (1820 g) from three-year-old palm tree were milled and homogenized in 7.28 L distilled water for 22-24 h at room temperature. Excess material was removed by vacuum filtration and centrifugation (10000*g*, 277 K for 15 min). Pigments were extracted by phase separation over 20-22 h at 277 K after the addition to the supernant of solid PEG to 14% (w/v) and solid ammonium sulfate to 10% (w/v). Two phases were formed after addition of ammonium sulfate: an upper polymer phase (dark brown), which contained pigments, phenols, polyphenols, oxidized phenols and PEG, and lower aqueous phase (yellow) containing peroxidase. Each phase consisted of 50% of the initial volume. These phases were separated and the phase containing peroxidase activity was centrifugated. The clear supernant containing peroxidase activity was titrated with ammonium sulfate to a conductivity value of 232 mS cm^{-1} and was applied on a Phenyl-Sepharose column (1.5 x 35 cm) equilibrated with 100 mM phosphate buffer, pH 6.5, with 1.7 M ammonium sulfate, which has the same conductivity as the sample. The enzyme was eluted with 100 mM phosphate buffer, pH 6.5, plus 0.2 M ammonium sulfate at a flow rate of 1 mL min^{-1}. 15 mL fractions were collected and those showing peroxidase activity were dialyzed against 5 mM Tris buffer, pH 9.3, for 72 h, with constant stirring at 277-278 K. these fractions were membrane-concentrated (Amicon, 10

kDa cutoff) to 15 mL and applied onto a TSK-Gel DEAE-5PW column (1 x 30 cm) equilibrated with 5 mM Tris buffer, pH 9.3. Elution was carried out with a linear 0-300 mM NaCl gradient in the same buffer at a flow rate of 1 mL min^{-1}. The fractions with peroxidase activity were collected, membrane-concentrated (Amicon, 10 kDa cutoff), and applied on a Superdex-200 column equilibrated with 5 mM Tris buffer, pH 9.3. Elution was carried out in the same buffer at a flow rate of 1 mL min^{-1}. Finally, the peroxidase was dialyzed against distilled water and freeze-dried.

The purity of the CEP was determined by SDS-PAGE as described by Fairbanks et al. [30] on a Bio-Rad Minigel device using a flat block with 12% polyacrylamide concentration; by gel filtration, which was performed using a Superdex 200 10/30 HR column in an FPLC Amersham Äkta System; and by UV-visible spectrophotometry ($RZ = A_{403}/A_{280} = 2.8 – 3.0$). Analytical isoelectrofocusing was performed on a Mini IEF cell model 111 (Bio-Rad Laboratories, Hercules, CA, USA) using Ampholine PAG-plates, pH 3.5-9.5 (GE Healthcare Biosxiencies AB, Upsala, Sweden). The electrophoretic conditions and Silver Staining Kit Protein were as recommended by manufacturer. The standards used were from a broad-range p*I* calibration kit (4.45-9.6) from Bio-Rad Laboratories (Hercules, CA, USA.).

2.3. Enzymatic activity of CEP

The initial rates of appearance of the products of oxidation of different substrates (guaiacol, ABTS (2,2'-azino-bis(3-ethylbenzthiazoline-6-sulphonic acid), o-dianisidine and o-phenylendiamine) due to the catalytic action of CEP in the presence of H_2O_2 were measured by electronic absorption spectroscopy at the characteristic wavelengths of such products (470, 414, 420 and 445 nm, respectively) [31]. The reactions, initiated by the addition of CEP, were performed at 25 ^{o}C in 20.0 mM universal buffer, pH 7.0 except for substrate ABTS for which

pH was 3.0, containing variable concentrations of the reducing substrate at fixed H_2O_2 concentration and *viceversa*.

The concentration of peroxidase was measured spectrophometrically at 403 nm, using the experimentally determined extinction coefficient value of 48.0 ± 0.5 mM^{-1} cm^{-1} for the protein monomer [17].

To determine the microscopic rate constants and other kinetic parameters for the oxidation of the substrates by CEP in the presence of H_2O_2, the mathematical treatment of Morales and Ros-Barceló [32] was applied. The initial reaction rates were obtained from the kinetic runs and fitted *vs.* substrate concentration, at fixed H_2O_2 concentration, and *viceversa*, according to the generally accepted two-substrate Ping-Pong mechanism for the peroxidases [19,20].

3. Results and discussion

3.1. Steady-state rate equation and kinetic parameters of CEP-catalyzed oxidation reactions

In a two-substrate enzyme system, two general mechanisms are possible for the interaction of the substrates with the enzyme: namely, a sequential mechanism or a Ping-Pong mechanism. In a sequential mechanism, both substrates combine with the enzyme to form a ternary complex before catalysis occurs. The substrates can combine with the enzyme in a random fashion (Random Bi-Bi) or in an obligatory order (Ordered Bi-Bi) to form the ternary complex. The products formed from the reaction can therefore be released in an ordered or random fashion. In a Ping-Pong mechanism, a ternary complex of substrates and enzyme is not formed. The first substrate in a Bi-Bi Ping-Pong mechanism combines with the enzyme to form a substituted enzyme intermediate, with the concomitant release of the first product. The second substrate then interacts with the substituted enzyme intermediate to form the second product and regenerate the native enzyme. Ping-Pong and sequential mechanisms can be differentiated

by a steady-state kinetic analysis of the reaction using the procedures described by Cleland [33,34].

The kinetic mechanism of the H_2O_2-assisted CEP-catalyzed oxidation of reducing substrates AH_2 was investigated using initial rate measurements, in which the concentrations of both substrates, - H_2O_2 and AH_2 - were varied systematically and the results were analyzed assuming steady state conditions. The initial rates, v, as a function of hydrogen peroxide or AH_2 concentration were fitted to the Michaelis-Menten rate equation (Eq. (A2)) by an iterative process [35].

At pH 3.0, double-reciprocal plots of initial steady-state rates of ABTS oxidation *vs.* hydrogen peroxide concentration (0.1-2.1 mM), at fixed reducing substrate ABTS concentrations, afforded a set of approximately parallel lines, as show in Figure 1. A similar graphic behaviour of the double-reciprocal plots of the data was obtained upon studying the effect of ABTS concentrations on the initial rates of the oxidation reaction at different fixed H_2O_2 concentrations (data not shown). Similar trends towards parallel lines in double-reciprocal plots were also observed at pH 7.0 for guaiacol, o-dianisidine and o-phenylendiamine. The obtained trends towards such linear parallel plots point to a Ping-Pong mechanism involving two independent enzyme forms (i.e. enzyme forms separated by an irreversible step).

Figure 1

Thus, upon representing the intercept (1/V) of the above lines and the inverse of the *K* parameter *vs.* the reciprocal of the fixed substrate concentration, linear relationships are obtained (insets in Figure 1 for the ABTS case). The values of $K_m^{H_2O_2}$, $K_m^{AH_2}$ V_{max} and k_{cat}, shown in Table 1, were calculated from the slopes and intercepts of the corresponding linear fittings of data following equations (A6) and (A7).

Table 1

The highest turnover number, k_{cat}, of CEP was found for the substrate guaiacol, followed by o-phenylenediamine, o-dianisidine and ABTS. The highest affinity of the enzyme ($1/K_m$) was for ABTS, followed by o-phenylenediamine, o-dianisidine and guaiacol. However, the greatest specificity constant or catalytic efficacy of the enzyme (k_{cat}/K_m) was seen for ABTS, followed by o-phenylenediamine, o-dianisidine and guaiacol. Similar reactivities for these substrates have been found for African [31] and royal [18] palm tree peroxidases.

3.2. Microscopic rate constants

Peroxidases catalyzed the oxidation of AH_2 organic substrates, using H_2O_2 (or other peroxides) as electron acceptor, in a three-step catalytic cycle involving different intermediate enzyme forms [19,20]:

$$E + H_2O_2 \xrightarrow{k_1} EI + H_2O \quad (1)$$

$$EI + AH_2 \xrightarrow{k_2} EII + AH^{\bullet} \quad (2)$$

$$EII + AH_2 \xrightarrow{k_1} E + H_2O + AH^{\bullet} \quad (3)$$

where E is the native enzyme. The monoelectronic oxidation of the native state E gives rise to an intermediate state termed EI (Eq. (1)). EI is responsible for the oxidation of the electron-donor substrate (AH_2), accepting one proton and one electron, and generating its free radical ($AH^{\bullet}$) and another enzyme state, designated EII (Eq. (2)). Finally, EII is reduced by a second molecule of substrate (Eq. (3)), giving rise to a second free radical ($AH^{\bullet}$). The microscopic constant k_1 (the constant of EI formation) indicates the reactivity of the enzyme towards hydrogen peroxide and k_3 (the constant of EII reduction) represents the reactivity of the enzyme towards the reducing substrate.

To calculate the microscopic constants (k_1 and k_3) for the oxidation of the substrates by CEP, the rates of oxidation of the substrates were fitted for each concentration of AH_2 and H_2O_2, assuming the steady-state approach and considering that $k_2 > k_3$.

Following the Appendix, double-reciprocal plots (1/v *vs.* 1/[H_2O_2]) allowed us to calculate A and B values for each AH_2 concentration. Figure 2 shows the plot of A *vs.* B values (Eq. (A8)) for three ABTS concentrations. From this straight line it is possible to calculate the value of k_1 (formation constant of compound I) for peroxidase-mediated ABTS oxidation. The value obtained, as well as those obtained for guaiacol, o-dianisidine and o-phenyldiamine are shown in Table 2.

Figure 2

Figure 3

According to the Appendix, double reciprocal plots (1/v *vs.* 1/[AH_2]) allowed us to calculate the A and B values (Eq. (A9)) for each H_2O_2 concentration. Figure 3 shows the plot of A *vs.* B values for three H_2O_2 concentrations during the oxidation of ABTS. From this straight line it is possible to calculate the value of k_3 (formation constant of compound II) for peroxidase-mediated ABTS oxidation. The value obtained, as well as those obtained for guaiacol, o-dianisidine and o-phenylenediamine are also listed in Table 2.

Table 2

These A *vs.* B plots allowed us to calculate true reaction constants (k_i) from steady-state measurements of the oxidation rate, avoiding their dependence on substrate concentration [20].

From the rate constant values (k_i) shown in Table 2, it may be deduced that the CEP is capable of oxidizing phenolic and aromatic amine substrates. The data obtained show that the most reactive substrate for CEP was ABTS, followed by the aromatic amines o-dianisidine and

o-phenylendiamine, guaiacol being the least reactive substrate. The high reactivity of ABTS is due to its greater number of H-bond acceptor atoms, because the highest values of reactivity constants are for substrates with the most acceptor H-bonds (www.chemicalregister.com). ABTS has ten H-bond acceptor sites, o-dianisidine four, o-phenylendiamine two and guaiacol two. With regards to H-bond acceptor sites - ABTS, o-dianisidine, o-phenylendiamine - each has two H-bond donor sites and guaiacol only one.

Similar studies addressing kinetic parameters and microscopic rate constants carried out with African [31] and Royal [18] palm tree peroxidases revealed that these enzymes exhibit greater reactivity towards ferulic acid and ABTS, followed by the aromatic amines o-dianisidine, o-phenylendiamine and, finally, by phenolic substrates with one or two hydroxyl groups in their chemical structures. In contrast, both soybean and peanut peroxidases are more reactive towards guaiacol than towards amines [31,36]. Both horseradish and tobacco peroxidases have been reported to be equally reactive towards guaiacol and o-dianisidine and about 10-15 times less reactive towards o-phenylendiamine [37].

Substrate specificity studies of peroxidases are usually performed with only one substrate present, besides H_2O_2, in the reaction mixture at a given time; i.e. without any alternative substrates able to undergo the same reaction. This is because the presence of competing substrates tends to complicate the analysis without providing much more information than would be obtained by studying the substrates separately. However, this implies an important difference between experimental practice and the physiological conditions under which enzymes usually exist. In this sense, most enzymes are not perfectly specific for a single substrate and must often select between several that are available simultaneously. Therefore, to be physiologically meaningful enzyme specificity must be defined in terms of how well the enzyme can discriminate between substrates present in the same reaction mixture. This does not mean that it cannot be determined from the kinetic parameters of the enzyme for separate

substrates, but it does mean that these parameters need to be interpreted correctly and not on a casual basis [38].

3.3. Substrate inhibition

In order to further verify the kinetic mechanism of the substrate oxidation reactions catalyzed by CEP, inhibition studies were carried out. One of the characteristic features of Ping-Pong reaction mechanisms is the occurrence of competitive substrate inhibition by both substrates [29].

In the Ping-Pong reaction mechanism, since the three forms of the enzyme - E, CoI and CoII - are so similar, it is reasonable to expect AH_2 to have some affinity for E as well as CoI and CoII and, if the actives sites in CoI and CoII are not too full for the adsorption of H_2O_2, for H_2O_2 to show some affinity for CoI and CoII [39]. In peroxidases, the formation of a non-productive or dead-end complex between AH_2 and E and the reaction of high concentrations of H_2O_2 with CoI affording H_2O_2 and O_2 have been found [40].

According to the Appendix, following the reciprocal of equation (A13), plots of 1/v *vs.* $1/[H_2O_2]$ at fixed $[AH_2]$ should be linear and should intersect on the y axis. This graphical behaviour was observed at fixed ABTS inhibitory concentrations (Figure 4).

In this sense, Figure 4 (inset) shows this linear plot for ABTS. For the other substrates studied, a similar degree of substrate competitive inhibition was found (data not shown).

Figure 4

Alternatively, at fixed inhibitory values of H_2O_2 concentration, the v *vs.* $[AH_2]$ data analysis provided a series of alternative equations similar to equations (A13-A16).

Accordingly, the corresponding plots of 1/v *vs.* 1/[AH_2] at fixed [H_2O_2] are also linear and intersect on the y axis and the plots of *K*/V *vs.* [H_2O_2] should also be linear. This graphic behaviour was obtained for ABTS at fixed [H_2O_2] (Figure 5) and also for the rest of substrates studied (data not shown).

Figure 5

Consequently, competitive substrate inhibition was observed in the H_2O_2-assisted CEP-catalyzed oxidation reactions for both substrates, as expected for a Ping-Pong reaction mechanism. The corresponding inhibition constants obtained - $K_{SI}^{H_2O_2}$ and $K_{SI}^{AH_2}$ - for the substrates studied are shown in Table 3.

Table 3

Thus, the combined initial rate and substrate inhibition results exclude an ordered or random sequential reaction mechanism, and are only consistent with the Bi-Bi Ping-Pong mechanism following the notation of [29] as the minimal kinetic model for H_2O_2-assisted CEP-catalyzed substrate oxidation reactions.

Ping-Pong reaction kinetics has also been observed for several other peroxidase-catalyzed oxidations mediated by compound I. The results of initial rate studies of the hydrogen peroxide-supported oxidation of guaiacol by turnip peroxidase [41] and of the oxidation of ferrocytochrome c catalyzed by horseradish peroxidase [42] and yeast cytochrome c peroxidase [43] are consistent with a Ping-Pong mechanism. The initial rate kinetic studies of the oxidation of ferrocytochrome c by *Pseudomonas aeruginosa* cytochrome c peroxidase yielded intersecting plots, which were initially interpreted as indicating a sequential reaction mechanism [44]. However, subsequent studies demonstrated that the intersecting plots arose from the formation of an inactive hydrogen peroxide-enzyme complex, and the mechanism of

the reaction was reinterpreted to be of the modified Ping-Pong type [45]. Recently, it has been found that Royal palm tree peroxidase also exhibits a Bi-Bi Ping-Pong mechanism for the H_2O_2-assisted catalyzed oxidation reactions of o-dianisidine, o-phenylenediamine, ferulic acid, guaiacol and catechol [37].

Acknowledgments

Funding from Consejeria de Educación (projects SA129A07 and SA052A10-2) and Consejeria de Agricultura y Ganaderia (Project SA06000) of the Regional Government of Castilla and León (Junta de Castilla y León, Spain) is acknowledged.

References

[1] C. Penel, T. Gaspar, H. Greppin, Plant Peroxidases 1980-90. Topics and Detailed Literature on molecular, biochemical, and physiological aspects. University of Geneva, Switzerland, 1992.

[2] J.S. Dordick, M.A. Marletta, A.M. Klibanov, Biotech. Bioeng. 30 (1987) 31-36.

[3] J.A. Akkara, K.J. Senecal, D.L. Kaplan, J. Polym. Sci: Part A: Polymer Chem. 29 (1991) 1561-1574.

[4] R.Q. Thompson, Anal. Chem. 59 (1987) 1119-1121.

[5] Z. Weng, M. Hendrickx, G. Maesmans, P. Tobback, J. Food Sci. 56 (1991) 574-578.

[6] D. Arseguel, M.J. Baboulène, J. Chem. Technol. Biotechnol. 61 (1994) 331-335.

[7] P.R. Adler, R. Arora, A. El Ghaouth, D.M. Glenn and J.M. Solar, J. Environ. Qual. 23 (1994) 1113-1117.

[8] L.S. Zamorano, M.G. Roig, E. Villar, V.L. Shnyrov, Cur. Top. Biochem. Res. 9 (2007) 1-26.

[9] H.B. Dunford, Heme Peroxidases, John Wiley & Sons, Inc., New York, 1999.

[10] D.J. Schuller, N. Ban, R.B. van Huystee, A. McPherson, T.L. Poulos, Structure 4 (1996) 311-321.

[11] C.B. Rasmussen, A.N. Hiner, A.T. Smith, K.G. Welinder, J. Biol. Chem. 273 (1998) 2232-2240.

[12] M. Kvaratskhelia, C. Winkel, R.N. Thorneley, Plant Physiol. 114 (1997) 1237-1245.

[13] L. Ostergaard, A.K. Abelskov, O. Mattsson, K.G. Welinder, FEBS Lett. 398 (1996) 243-247.

[14] A. Rodríguez, D.G. Pina, B. Yélamos, J.J. Castillo León, G.G. Zhadan, E. Villar, F. Gavilanes, M.G. Roig, I.Y. Sakharov, V.L. Shnyrov, Eur. J. Biochem. 269 (2002) 2584-2590.

[15] L. Watanabe, A.S. Nascimiento, L.S. Zamorano, V.L. Shnyrov, I. Polikarpov, Acta Cryst. F63 (2007) 780-783.

[16] L.S. Zamorano, D.G. Pina, J.B. Arellano, S.A. Bursakov, A.P. Zhadan, J.J. Calvete, L. Sanz, P.R. Nielsen, E. Villar, O. Gavel, M.G. Roig, L. Watanabe, I. Polikarpov, V.L. Shnyrov, Biochimie 90 (2008) 1737-1749.

[17] L.S. Zamorano, S.B. Vilarmau, J.B. Arellano, G.G. Zhandan, N. Hidalgo-Cuadrado, S.A. Bursakov, M.G. Roig, V.L. Shnyrov, Int. J. Biol. Macromol. 44 (2009) 326-332.

[18] L. Watanabe, P. Ribeiro de Moura, L. Bleicher, A.S. Nascimiento, L.S. Zamorano, J.J. Calvete, L. Sanz, A. Pérez, S. Bursakov, M.G. Roig, V.L. Shnyrov, I. Polikarpov, J. Struct. Biol. 169 (2009) 226-242.

[19] T.L. Poulos, J. Kraut, J. Biol. Chem. 255 (1980) 8199-8205.

[20] C.B. Rasmussen, H.B. Dunford, K.G. Welinder, Biochemistry 34 (1995) 4022-4029.

[21] J.N. Rodriguez-López, D.L. Lowe, J. Hernández-Ruiz, A.N.P. Hiner, F. Garcia-Cánovas, R.N.F. Thorneley, J. Am. Chem. Soc. 123 (2001) 11838-11847.

[22] H.B. Dunford, J.S. Stillman, Coord. Chem. Rev. 19 (1976) 187-251.

[23] W. Wang, S. Noël, M. Desmadril, J. Guéguen, T. Michons, Biochem. J. 340 (1999) 329-336.

[24] R.E. Childs, W.G. Bardsley, Biochem. J. 145 (1975) 93-103.

[25] G. Wolters L. Kuijpers J. Kacaki, A. Schuurs, J. Clin. Pathol. 29 (1976) 873-879.

[26] J.H. Bovaird, T.T. Ngo, H.M. Lenhoff, Clinical Chemistry, 28 (1982) 2423-2426.

[27] P. Tijssen, Practice and Theory of Enzyme Immunoassays, Elsevier Science Ltd., 1985.

[28] Q.G. Jiao, A. Onwuegbuzie, A. Lichtenstein, Library and Information Science Research. 18 (1996) 150-163.

[29] W.W. Cleland, The Enzymes (P.D. Boyer, ed.) Academic Press, New York, 1970

[30] G. Fairbanks, T.L. Steck, D.F.H. Wallach, Biochemistry 10 (1971) 2606-2617.

[31] I.Y. Sakharov, B.M.K. Vesga, I.V. Sakharova, Biochemistry (Moscow) 67 (2002) 1043-1047.

[32] M. Morales, A. Ros-Barceló, Phytochemistry 45 (1997) 229-232

[33] W.W. Cleland, Biochim. Biophys. Acta 67 (1963) 104-137.

[34] W.W. Cleland, Biochim. Biophys. Acta 67 (1963) 173-187.

[35] W.W. Cleland, Methods Enzymol. 63 (1979) 103-138.

[36] I.G. Gazaryan, L.M. Lagimini, G.A. Ashby, R.N.F. Thorneley, Biochem. J. 313 (1996) 841-847.

[37] L.S. Zamorano, Physicochemical characterization of royal palm tree (*Roystonea regia* L.) peroxidase, an enzyme with high stability. Ph.D. Thesis, School of Chemistry, University of Salamanca (Spain) (2009) 174-190.

[38] A. Cornish-Bowden, Fundamentals of Enzyme kinetics, Portal Press Ltd, London, 1995

[39] W.W. Cleland, Methods Enzymol. 63 (1979) 500-513.

[40] A.N.P. Hiner, L. Sidrach, S. Chazarra, R. Varón, J. Tudela, F. Garcia-Cánovas, J.N. Rodríguez-López, Biochimie 86 (2004) 667-676.

[41] T. Hosoya, J. Biochem. 47 (1960) 369–381.

[42] M. Santimone, Biochimie 57 (1975) 91-96.

[43] T. Yonetani, G.S. Ray, J. Biol. Chem. 241 (1966) 700-706.

[44] M. Ronnberg, N. Ellfolk, Acta Che. Scand. B. 29 (1975) 719-727.

[45] M. Ronnberg, T. Araiso, N. Ellfolk, H.B. Dunford, J. Biol. Chem. 256 (1981) 2471-2474.

Figure legends

Fig. 1. Primary double-reciprocal plot of the initial rate of ABTS oxidation as a function of hydrogen peroxide concentration at fixed ABTS concentrations (0.032 mM (□), 0.04 mM (○), 0.05 mM (Δ)). The inserts show the secondary plots of 1/V *vs.* 1/[ABTS] (a) and of 1/K *vs.* 1/[ABTS] (b). See text for other experimental conditions.

Fig. 2. Secondary plot of parameters A (nmol s^{-1}) *vs.* B (mM) obtained by varying H_2O_2 concentrations for three ABTS concentrations (0.032, 0.04, 0.05 mM). See text for other experimental conditions.

Fig. 3. Secondary plot of parameters A (nmol s^{-1}) *vs.* B (mM) obtained by varying ABTS concentrations for three H_2O_2 concentrations (1.2, 1.6, 2.1 mM). See text for other experimental conditions.

Fig. 4. Primary double-reciprocal plot of the initial rate of ABTS oxidation as a function of ABTS concentration at fixed hydrogen peroxide inhibitory concentrations (0.12 mM (□), 0.4 mM (○), 0.6 mM (Δ)). The insert shows the secondary plot of K/V *vs.* H_2O_2 concentration. See text for other experimental conditions.

Fig. 5. Primary double-reciprocal plot of the initial rate of ABTS oxidation as a function of hydrogen peroxide concentration at fixed ABTS inhibitory concentrations (0.32 mM (□), 0.4 mM (○), 0.5 mM (Δ)). The insert shows the secondary plot of K/V *vs.* ABTS concentration. See text for other experimental conditions.

APPENDIX

The rate equation for an enzyme-catalyzed Ping-Pong reaction with two substrates, H_2O_2 and AH_2, in the absence of products and at non-inhibitory substrate concentrations, is given by

$$v = \frac{V[H_2O_2]\,[AH_2]}{K_m^{H_2O_2}[AH_2] + K_m^{AH_2}[H_2O_2] + [H_2O_2]\,[AH_2]} \quad \text{(A1)}$$

which can be cast in the form of a rectangular hyperbola for fixed values of $[AH_2]$:

$$v = \frac{V[H_2O_2]}{K + [H_2O_2]} \quad \text{(A2)}$$

where V and *K* parameters are as follows:

$$V = \frac{V_{max}}{1 + \frac{K_m^{AH_2}}{[AH_2]}} \quad \text{(A3)}$$

$$K = \frac{K_m^{H_2O_2}}{1 + \frac{K_m^{AH_2}}{[AH_2]}} \quad \text{(A4)}$$

Thus plots of 1/v *vs.* $1/[H_2O_2]$ are linear and parallel at different fixed $[AH_2]$ since:

$$\frac{1}{v} = \frac{1}{V} + \frac{K}{V[H_2O_2]} \quad \text{(A5)}$$

Furthermore, the reciprocals of equations (A3) and (A4) are given by:

$$\frac{1}{V} = \frac{1}{V_{max}} + \frac{K_m^{AH_2}}{V_{max}} \frac{1}{[AH_2]} \quad \text{(A6)}$$

$$\frac{1}{K} = \frac{1}{K_m^{H_2O_2}} + \frac{K_m^{AH_2}}{K_m^{H_2O_2}} \frac{1}{[AH_2]} \quad (A7)$$

For non-inhibitory concentrations of H_2O_2, the initial rates of the substrate oxidation can be fitted to the following equation:

$$v = \frac{A[H_2O_2]}{B + [H_2O_2]} \quad (A8)$$

where A = 2[E]k_3[AH_2] and B=(k_3/k_1)[AH_2]. Double-reciprocal plots (1/v *vs.* 1/[H_2O_2]) allowed us to calculate A and B values for each AH_2 concentration

Similarly, the dependence of v on [AH_2] may be written as:

$$v = \frac{A[AH_2]}{B + [AH_2]} \quad (A9)$$

where A = 2[E]k_1[H_2O_2] and B = (k_1/k_3)[H_2O_2]. Double reciprocal plots (1/v *vs.* 1/[AH_2]) allowed us to calculate the A and B values for each H_2O_2 concentration

From equation (A8), the catalytic efficacy for the utilization of H_2O_2 would be given by:

$$\frac{k_{cat}}{K_m^{H_2O_2}} = \frac{2k_3[AH_2]}{(k_3/k_1)[AH_2]} = 2k_1 \quad (A10)$$

while the catalytic efficacy for the utilization of the substrate AH_2 would be given by:

$$\frac{k_{cat}}{K_m^{AH_2}} = \frac{2k_1[H_2O_2]}{(k_1/k_3)[H_2O_2]} = 2k_3 \quad (A11)$$

Consequently, the reactivity of the enzyme with hydrogen peroxide is determined by the value of the constant k_1. However, its reactivity with the reducing substrate is determined by the constant k_3.

The occurrence of competitive substrate inhibition by both substrates in the reaction mechanism means that in the denominator of the rate equation (A1), the $K_m^{H_2O_2}[AH_2]$ term can be multiplied by $\left(1+[AH_2]/K_{IS}^{AH_2}\right)$ and the $K_m^{AH_2}[H_2O_2]$ term by $\left(1+[H_2O_2]/K_{IS}^{H_2O_2}\right)$ where $K_{IS}^{AH_2}$ and $K_{IS}^{H_2O_2}$ are the dissociation constants of AH_2 from EAH_2 and of H_2O_2 from CoI H_2O_2 and/or CoII H_2O_2 complexes, respectively, (Eq. (A15)), and double competitive substrate inhibition would be exhibited when AH_2 and H_2O_2 are varied. Thus, the corresponding rate equation would be:

$$v = \frac{V[H_2O_2][AH_2]}{K_m^{H_2O_2}[AH_2]\left(1+[AH_2]/K_{IS}^{AH_2}\right)+K_m^{AH_2}[H_2O_2]\left(1+[H_2O_2]/K_{IS}^{H_2O_2}\right)+[H_2O_2][AH_2]} \quad \text{(A12)}$$

At fixed inhibitory values of the AH_2 concentration, the v *vs.* $[H_2O_2]$ data were fitted to the following rate equation of competitive inhibition:

$$v = \frac{V_{max}[H_2O_2]}{K_m^{H_2O_2}\left(1+\frac{[AH_2]}{K_{IS}^{AH_2}}\right)+[H_2O_2]} \quad \text{(A13)}$$

For competitive inhibition, the K and V of equation (A2) are defined by

$$V = \frac{V_{max}}{1+\frac{K_m^{AH_2}}{[AH_2]}} \quad \text{(A14)}$$

$$K = \frac{K_{m}^{H_2O_2}\left(1+\frac{[AH_2]}{K_{IS}^{AH_2}}\right)}{1+\frac{K_{m}^{AH_2}}{[AH_2]}} \quad \text{(A15)}$$

Thus, following the reciprocal of equation (A13), plots of 1/v *vs.* 1/[H_2O_2] at fixed [AH_2] should be linear and should intersect on the y axis.

Furthermore, the plots of *K*/V *vs.* [AH_2] should be linear because

$$\frac{K}{V} = \frac{K_{m}^{H_2O_2}}{V} + \frac{K_{m}^{H_2O_2}[AH_2]}{K_{IS}^{AH_2}V_{max}} \quad \text{(A16)}$$

Table 1

Kinetic parameters obtained for the H_2O_2-mediated oxidation of substrates by CEP. See text for experimental conditions.

Substrate	$K_m^{H_2O_2}$ (M)	$K_m^{AH_2}$ (M)	V_{max} (Ms^{-1})	$[E_0]/10^8$ (M)	k_{cat} (s^{-1})	$k_{cat}/K_m^{H_2O_2}$ ($M^{-1}s^{-1}$)	$k_{cat}/K_m^{AH_2}$ ($M^{-1}s^{-1}$)
ABTS	$7.10 \cdot 10^{-5}$	$6.15 \cdot 10^{-4}$	$1.07 \cdot 10^{-4}$	9.19	$1.16 \cdot 10^{3}$	$1.63 \cdot 10^{7}$	$1.89 \cdot 10^{6}$
Guaiacol	$3.58 \cdot 10^{-3}$	$9.25 \cdot 10^{-3}$	$8.39 \cdot 10^{-4}$	9.19	$9.13 \cdot 10^{3}$	$2.55 \cdot 10^{6}$	$9.87 \cdot 10^{5}$
o-dianisidine	$3.25 \cdot 10^{-3}$	$6.77 \cdot 10^{-3}$	$3.24 \cdot 10^{-4}$	9.19	$3.52 \cdot 10^{3}$	$1.08 \cdot 10^{6}$	$1.08 \cdot 10^{6}$
o-phenylendiamine	$9.26 \cdot 10^{-4}$	$3.03 \cdot 10^{-3}$	$5.06 \cdot 10^{-4}$	9.19	$5.51 \cdot 10^{3}$	$5.96 \cdot 10^{6}$	$1.82 \cdot 10^{6}$

Table 2

k_1 (μM^{-1} s^{-1}) and k_3 (μM^{-1} s^{-1}) values at 25 ºC for the H_2O_2-mediated oxidation of substrates by the CEP. See text for experimental conditions.

Substrate	k_1	k_3
ABTS	1.29	4.35
Guaiacol	0.45	0.01
o-dianisidine	0.15	0.27
o-phenylendiamine	0.19	0.05

Table 3

Competitive substrate inhibition constants.

Substrate	$K_{SI}^{H_2O_2}$ (M)	$K_{SI}^{AH_2}$ (M)
ABTS	$7.71 \cdot 10^{-4}$	$6.56 \cdot 10^{-8}$
Guaiacol	$4.39 \cdot 10^{-3}$	$1.31 \cdot 10^{-3}$
o-dianisidine	$3.77 \cdot 10^{-4}$	$2.13 \cdot 10^{-3}$
o-phenylendiamine	$8.78 \cdot 10^{-3}$	$4.56 \cdot 10^{-4}$

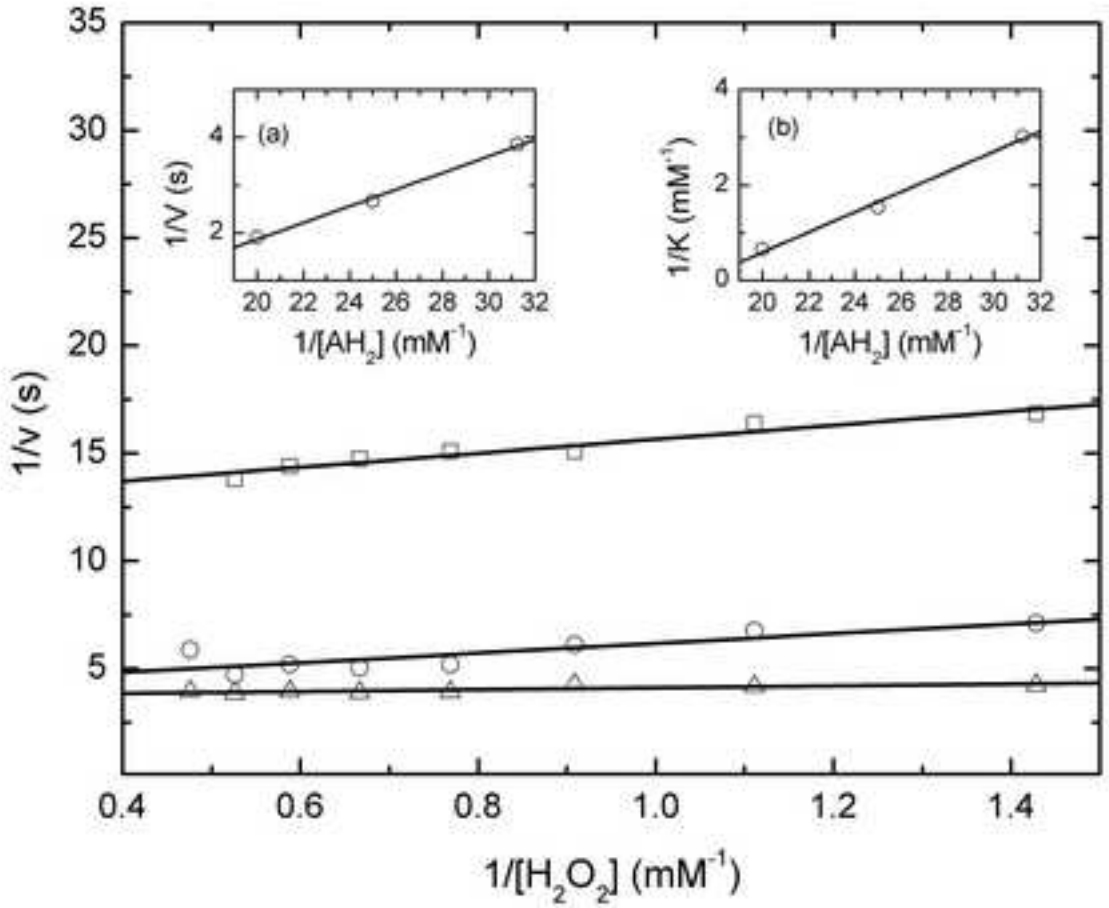

Fig 2

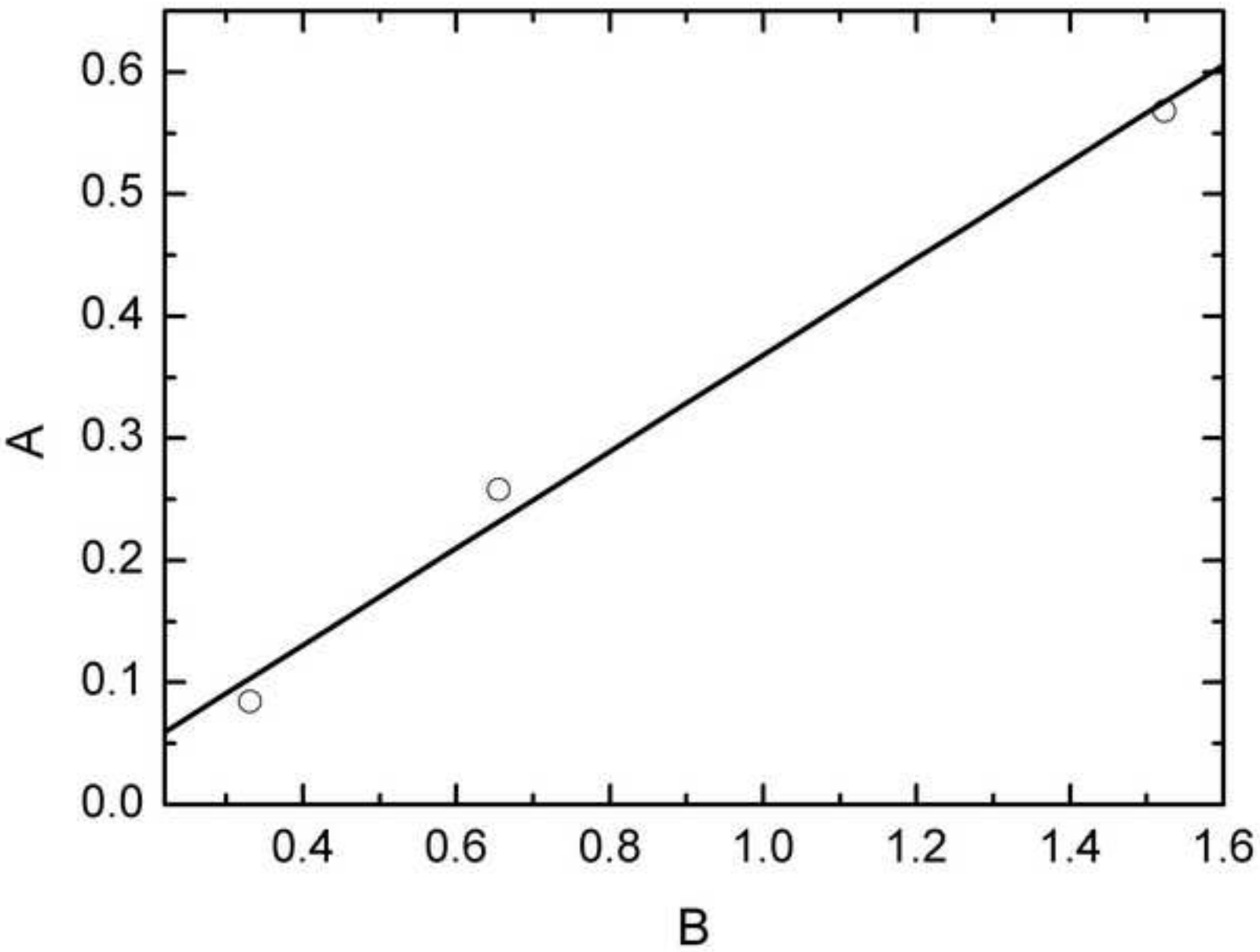

Fig 3

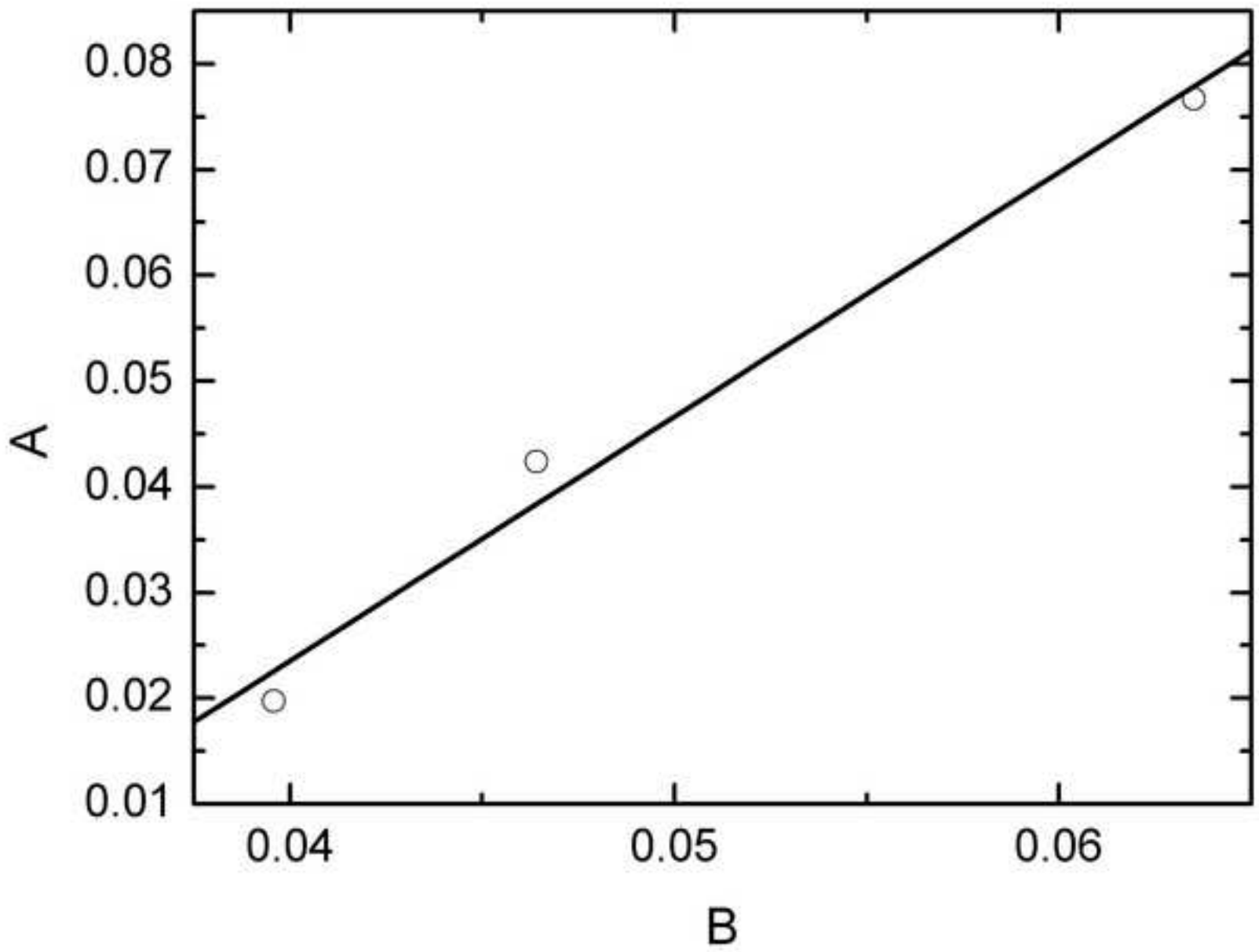

Figure4

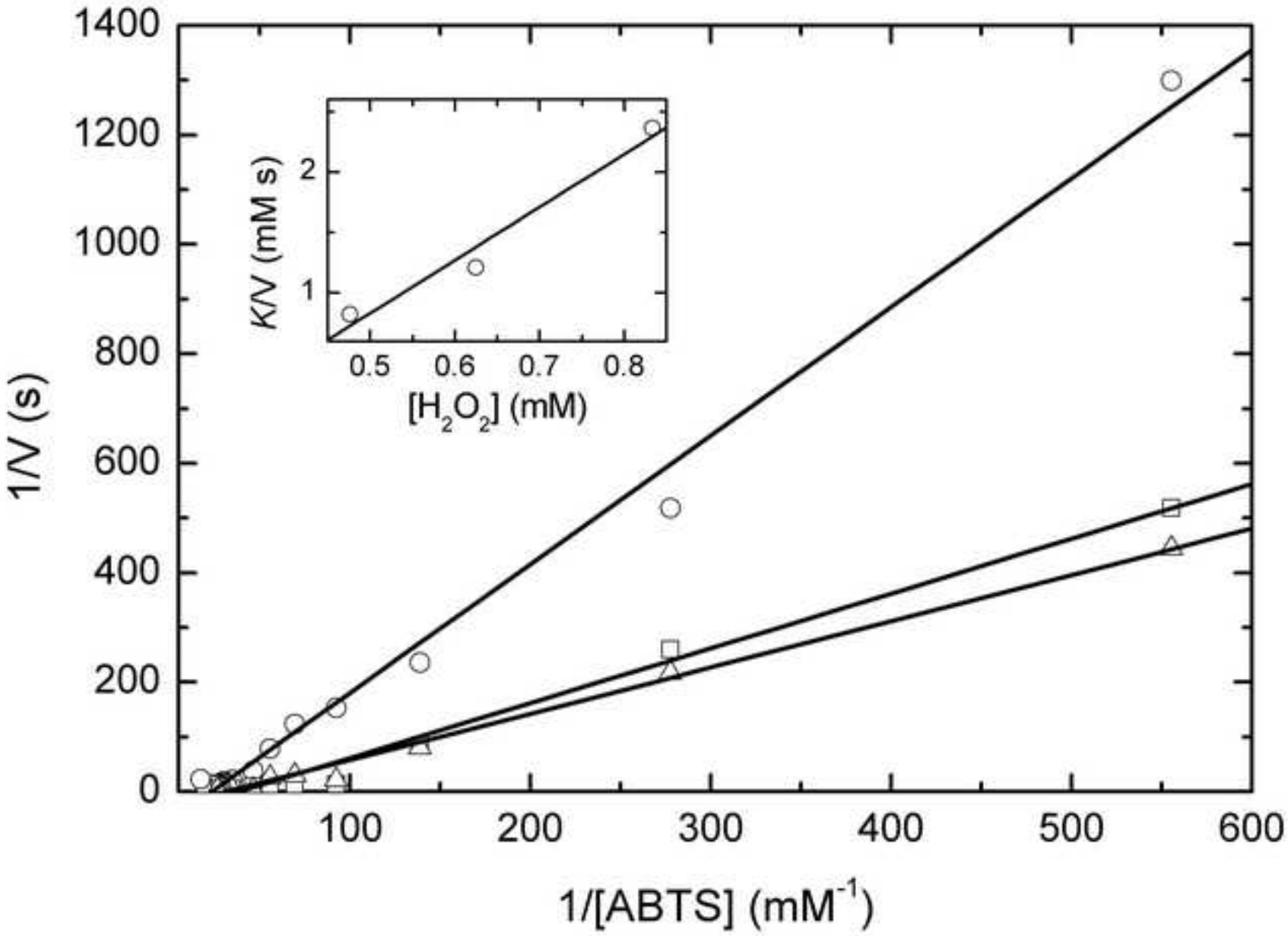
1400
1200
1000
800
600
400
200
0
1/V (s)
100
200
300
400
500
600
1/[ABTS] (mM-1)
K/V (mM s)
2
1
0.5
0.6
0.7
0.8
[H2O2] (mM)

Fig 5

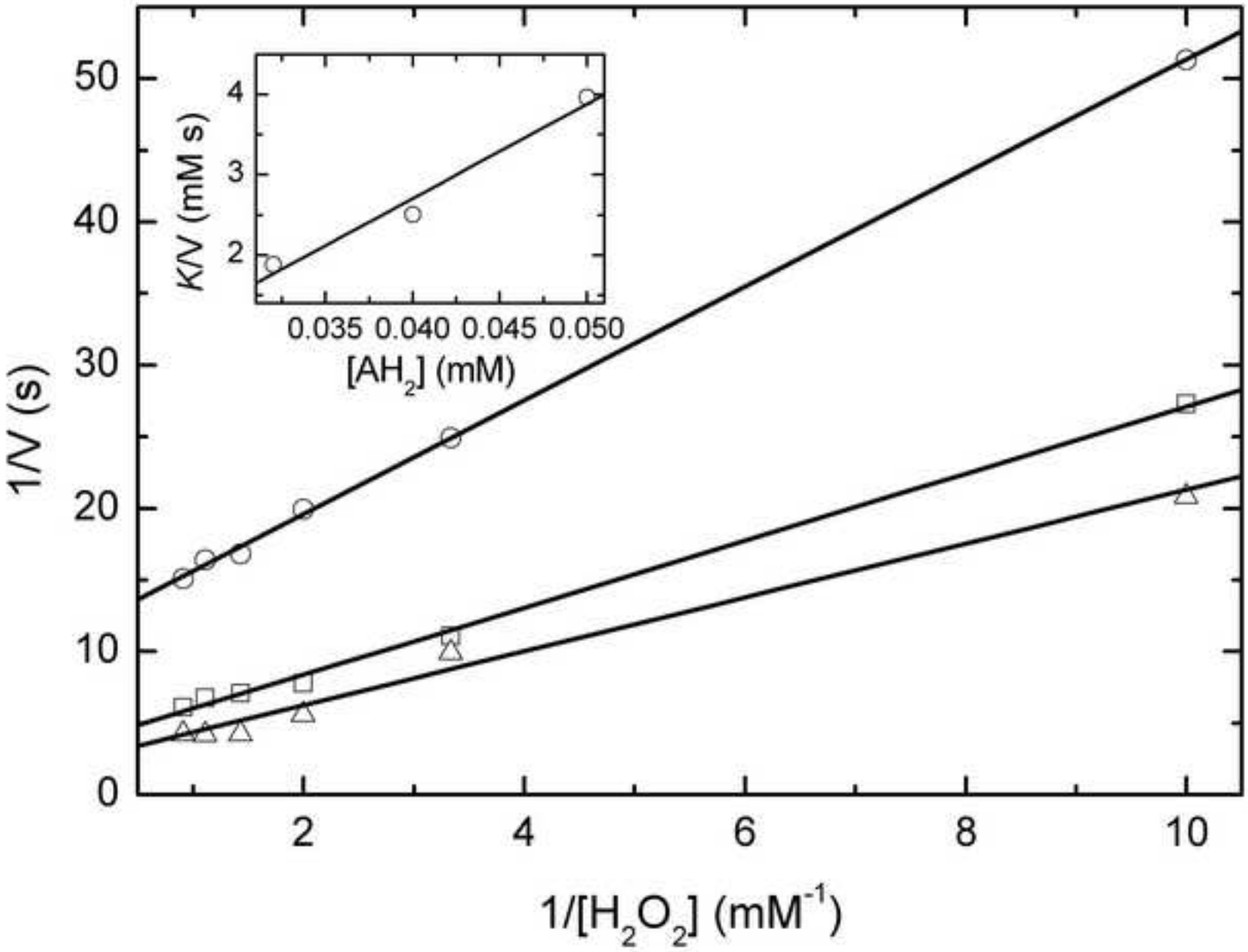
1/V (s)
1/[H2O2] (mM-1)
K/V (mM s)
[AH2] (mM)
0
10
20
30
40
50
2
4
6
8
10
2
3
4
0.035 0.040 0.045 0.050